Quantitation of protein–protein interactions by thermal stability shift analysis

Curtis J. Layton[1,2] and Homme W. Hellinga[1]*

[1]Department of Biochemistry, Duke University Medical Center, Durham, North Carolina 27710
[2]Program in Computational Biology and Bioinformatics, Duke University Medical Center, Durham, North Carolina 27710

Received 15 April 2011; Accepted 31 May 2011
DOI: 10.1002/pro.674
Published online 14 June 2011 proteinscience.org

Abstract: Thermal stability shift analysis is a powerful method for examining binding interactions in proteins. We demonstrate that under certain circumstances, protein–protein interactions can be quantitated by monitoring shifts in thermal stability using thermodynamic models and data analysis methods presented in this work. This method relies on the determination of protein stabilities from thermal unfolding experiments using fluorescent dyes such as SYPRO Orange that report on protein denaturation. Data collection is rapid and straightforward using readily available real-time polymerase chain reaction instrumentation. We present an approach for the analysis of the unfolding transitions corresponding to each partner to extract the affinity of the interaction between the proteins. This method does not require the construction of a titration series that brackets the dissociation constant. In thermal shift experiments, protein stability data are obtained at different temperatures according to the affinity- and concentration-dependent shifts in unfolding transition midpoints. Treatment of the temperature dependence of affinity is, therefore, intrinsic to this method and is developed in this study. We used the interaction between maltose-binding protein (MBP) and a thermostable synthetic ankyrin repeat protein (Off7) as an experimental test case because their unfolding transitions overlap minimally. We found that MBP is significantly stabilized by Off7. High experimental throughput is enabled by sample parallelization, and the ability to extract quantitative binding information at a single partner concentration. In a single experiment, we were able to quantify the affinities of a series of alanine mutants, covering a wide range of affinities (~ 100 n*M* to ~ 100 μ*M*).

Keywords: protein–protein interactions; thermal stability shifts; SYPRO Orange; binding assay; protein engineering

Introduction

Protein–protein interactions (PPIs) play a critical role in many biological processes.[1,2] Quantitative measurement of the interaction between binding partners is essential for analyzing biological systems,[3,4] discovering new therapeutics that disrupt PPIs,[5,6] and understanding the biophysical principles of these interactions.[7–9] Accurate quantitation of protein–protein binding remains one of the more difficult measurements in experimental biothermodynamics. The majority of quantitative methods determine dissociation constants (K_d) either from the kinetics of (dis)association[10,11] or from determination of the fraction of complex formed as a function of partner concentrations, for example, from changes in fluorescence[12–14] or heat[15,16] on complex formation or determination of the amount of free

Abbreviations: MBP, *Escherichia coli* maltose-binding protein; ORF, open reading frame; PPI, protein–protein interaction; RT-PCR, real-time polymerase chain reaction; SO, SYPRO Orange.

Additional Supporting Information may be found in the online version of this article.

Grant sponsor: NIH Director's Pioneer Award; Grant number: 5DPI OD000122.

*Correspondence to: Homme W. Hellinga, Department of Biochemistry, Duke University Medical Center, Box 3711, Durham, NC 27710. E-mail: hwh@biochem.duke.edu

partner.[17] Free energies are then derived by application of the well-known equation $\Delta G_b = RT\ln(K_d)$. A fundamentally different approach infers dissociation constants by exploiting the thermodynamic linkage between protein unfolding and ligand binding.[18–28] These methods determine the free energy of ligand binding by observing the ligand dependence of protein stability. They have the advantage of being able to measure a wide range of affinities (including high-affinity interactions that are otherwise difficult to measure) at a wide range of ligand concentrations (including concentrations well-above ligand saturation, which are not accessible by other methods). These methods were originally developed for measuring affinities between proteins and small molecules. In this study, we present their extension to the quantitation of PPIs.

The stabilities of proteins are changed (typically increased) upon addition of ligand. These changes are quantitatively linked to the affinity of the interaction. A particularly convenient technique to observe protein stability by thermal unfolding is based on the use of a dye that becomes fluorescent upon interaction with the unfolded state. The commercially available dye SYPRO Orange (SO)[29] is one such example, and it has excitation and emission properties compatible with readily available real-time polymerase chain reaction (RT-PCR) instrumentation.[19,20] High-throughput methodologies using small amounts of material have been developed to observe protein thermal denaturation using microtiter plates in RT-PCR instruments. For example, in this study, observations of protein unfolding made with SO were made in 384-well plates with sample volumes of 20 μL in each well. In these experiments, fraction of unfolded protein is monitored as an increase in fluorescence emission intensity of SO with temperature. The ligand dependence of stability is determined by measuring these profiles in the absence and presence of various ligand concentrations. From these observations, free energies of binding (and hence K_d) are extracted. In these experiments, data collection is straightforward and rapid, but quantitative analysis requires careful consideration of the underlying thermodynamic model and the dye-mediated reporting mechanism.

In this study, we demonstrate how PPIs can be measured by analysis of binding-induced shifts in multiprotein thermal transitions. We use the interaction between *Escherichia coli* maltose-binding protein (MBP) and the synthetic ankyrin-repeat protein Off7[30] as an experimental system to test our method. We show that the interaction between these two proteins can be detected through thermal stability shift and can be quantified by a thermodynamic model. We use interface mutants to demonstrate that a range of affinities can be analyzed in this manner.

Results

Ligand-induced shifts in stability for PPIs

Determination of affinities from ligand-induced shifts in stability exploits the linked equilibria between binding and folding. In the case of PPIs, the thermodynamic cycle describing such linkage relationships for two-state folding and single-site binding is a cube connecting eight states, because both partners can unfold and binding between all combinations of native and denatured states must be considered. For a single-site protein–protein association equilibrium is given as LMP + HMP ⇌ LMP-HMP (Scheme 1).

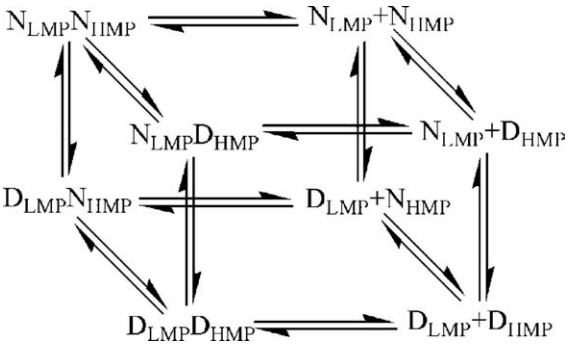

Scheme 1.

In Scheme 1, D_{LMP} is the denatured state of the partner with a lower melting temperature (lower melting partner, LMP), N_{HMP} is the native state of the higher melting partner (HMP), and D_xN_y are the various complexes between native (N) and denatured (D) states (x and y may be HMP or LMP). A powerful simplification can be made if there is sufficient separation in the melting temperatures (T_m values) of the two partners such that the LMP is predominantly unfolded before the HMP has begun its unfolding transition. If this condition applies, the HMP behaves as a stable ligand throughout the unfolding transition of the LMP. For analysis at temperatures well below the HMP unfolding transition, states containing D_{HMP} are unpopulated and the thermodynamic cycle reduces to the form given in Scheme 2.

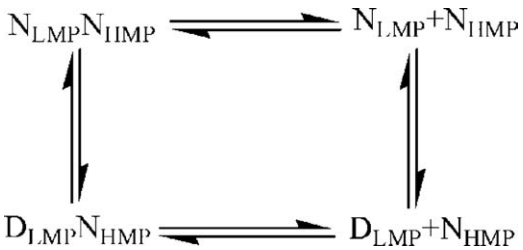

Scheme 2.

Under these conditions, binding can be analyzed solely in terms of HMP-induced shifts on the thermal stability of the LMP and is equivalent in many ways to the analysis of the interactions between proteins and non-protein ligands.[28] A further simplification can be made if binding interactions occur only between native states as shown in Scheme 3.

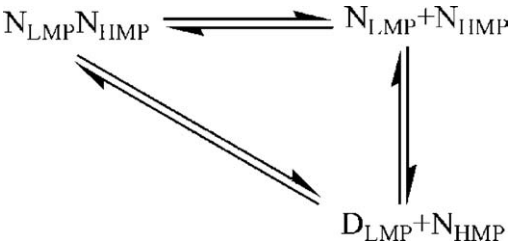

Scheme 3.

In this thermodynamic triangle, the binding free energy is just the difference in stability between apo and liganded protein. This model is used below to develop methods for data analysis.

To explore how much separation in the T_m values of the interacting partners is necessary to make the assumption leading to Scheme 2, the overlap of two (un)folding transitions can be simulated by calculating the fraction folded by both partners as a function of temperature. For a two-state model, the fraction (un)folded protein is given in Ref. 28:

$$f(T) = 1/1 + e^{-\left[\frac{\Delta_m H_u}{R}\left(\frac{1}{T}-\frac{1}{T_m}\right)\right]}, \quad (1)$$

where T_m is the midpoint temperature of the thermal unfolding transition, and $\Delta_m H_u$ is the enthalpy of unfolding at the T_m. The T_m difference necessary to achieve appropriate separation of the two folding transitions is dependent on the "steepness" of each transition, determined by the respective $\Delta_m H_u$ values of the partners [Fig. 1(A,B)]. For example, in order for 99% of the LMP to be denatured before 1% of the HMP is denatured, a ΔT_m of $\sim$ 15 to $\sim$ 20°C is required for $\Delta_m H_u$ values between 100 and 150 kcal/mol [Fig. 1(C)]. For 95% of the LMP to be denatured

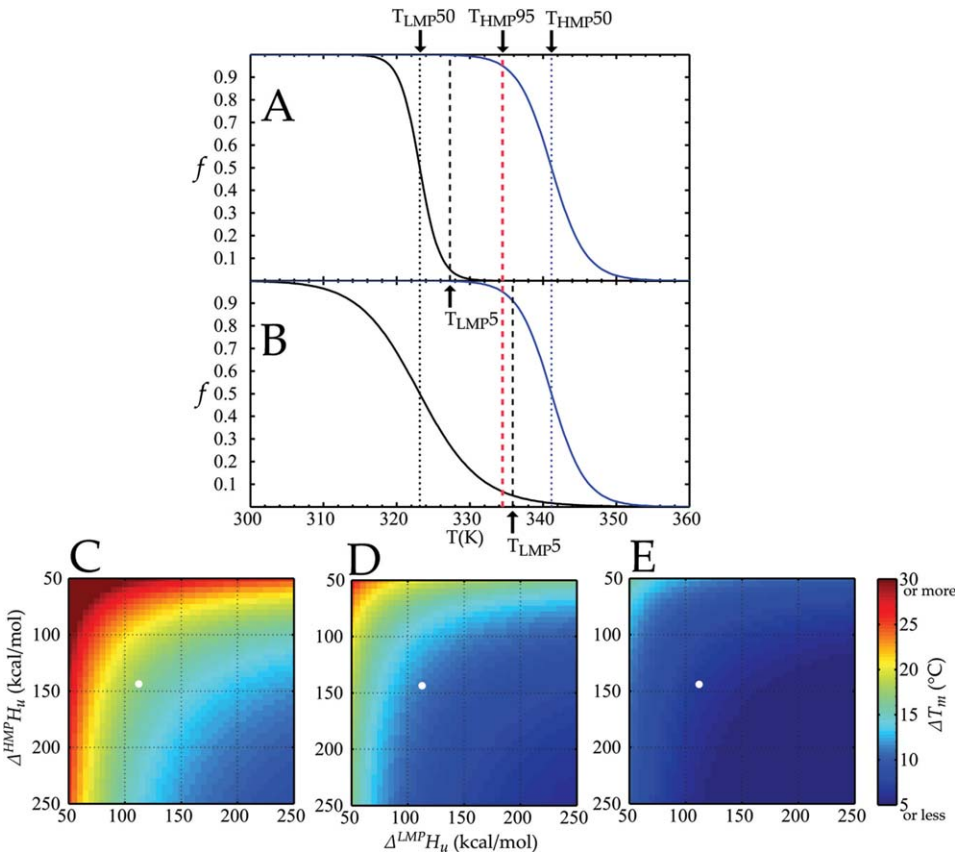

Figure 1. Simulated unfolding curves demonstrate potential overlap between two unfolding transitions. (A) Case 1: unfolding transitions for the lower melting partner (LMP) and higher melting partner (HMP) are well separated. The temperature at which only 5% of the LMP remains folded ($T_{LMP}5$) is significantly lower than the temperature at which 95% of the HMP is still folded ($T_{HMP}95$). The curves were simulated using Eq. (1) with: T_m of the LMP ($T_{LMP}50$), 50°C; $\Delta_{LMP}H_u$, 150 kcal/mol; T_m of the HMP ($T_{HMP}50$), 68°C; $\Delta_{HMP}H_u$, 100 kcal/mol. (B) Case 2: there is overlap between the unfolding transitions of the two partners, such that $T_{HMP}95 < T_{LMP}5$. Note that this change results from modulation of the unfolding enthalpy of the LMP, while the T_m of the LMP and all parameters for the HMP remain constant. Parameters for the simulation were $T_{LMP}50$, 50°C; $\Delta_{LMP}H_u$, 50 kcal/mol; $T_{HMP}50$, 68°C; $\Delta_{HMP}H_u$, 100 kcal/mol. (C–E) The required minimal separation values of the unfolding transition midpoints ($T_{HMP}50$ and $T_{LMP}50$) is dependent on the permitted overlap tolerance: (C) $T_{LMP}1 = T_{HMP}99$ (D) $T_{LMP}5 = T_{HMP}95$ (E) $T_{LMP}15 = T_{HMP}85$ ($T_{HMP}50 = 80$°C for C–E).

before 5% of the HMP is denatured, a ΔT_m of $\sim$ 8 to $\sim$ 12°C is required [Fig. 1(D)], and for 85% of the LMP to be denatured before 15% of the HMP is denatured, a ΔT_m of only $\sim$ 6 to $\sim$ 8°C is required over the same $\Delta_m H_u$ range [Fig. 1(E)]. This analysis applies to the T_m separation between the *ligand-shifted* LMP and the HMP; separation between melting transition temperatures of the apoproteins, therefore, must be greater, especially for high-affinity interactions.

Determination of PPI affinities

The above-mentioned analysis shows that under certain circumstances (Scheme 3), PPI affinities can be extracted from measuring the shifts in T_m values of the LMP in the presence of HMP, analogous to measuring ligand-dependent shifts in thermal stability. The binding free energy is simply the difference between the free energy of stability in the absence and presence of ligand:

$$\Delta G_b(T,[P],[L]) = \Delta^{apo}G_u(T) - \Delta^{L}G_u(T,[P],[L]), \quad (2)$$

where T is temperature, and $[P]$ and $[L]$ are the concentration of the LMP (the "protein") and the HMP (the "ligand"), respectively. The relevant protein thermal stabilities are determined at different temperatures because of the ligand-dependent perturbation of T_m. We, therefore, construct a thermodynamic model of the free energy of binding and stability as a function of both ligand and temperature. Such a model has been developed for the treatment of interactions between a single protein and a small molecule,[28] which extract both T_m and $\Delta_m H_u$ values from the experimental data. However, in the case of PPIs, $\Delta_m H_u$ cannot be fit with accuracy because the LMP post-transition baseline contains contributions from the HMP unfolding transition. We, therefore, present a modification of this previous treatment, in which $\Delta_m H_u$ now becomes a fit variable, rather than an experimental observable. We construct a master equation to achieve this aim and use it to quantitate protein–protein affinities from multiprotein thermal unfolding transitions.

The temperature dependence of protein stability in the absence of ligand is described by the Gibbs–Helmholtz relationship:

$$\Delta G_u(T) = \Delta_m H_u\left(1-\frac{T}{T_m}\right) - \Delta C_{p,u}\left(T_m - T + T\ln\left(\frac{T}{T_m}\right)\right), \quad (3)$$

where $\Delta_m H_u$ is the enthalpy of unfolding at the transition midpoint (T_m) and $\Delta C_{p,u}$ is the heat capacity of unfolding.

The concentration dependence of the free energy of stability is given by a rearrangement of Eq. (2):

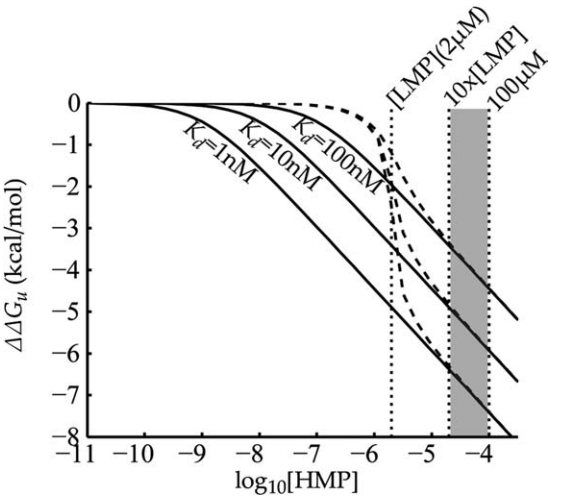

Figure 2. Simulations illustrating the shift in stability with binding partner concentration in the nonstoichiometric [solid line, Eq. (6)] and stoichiometric regime [dashed line, Eq. (7)] for different binding affinities (K_d values indicated). The stoichiometric regime was simulated with a [P] (LMP) of 2 μ*M*. Assuming a lower concentration limit of 10 × [P] = 20 μ*M* and a practical upper limit of 100 μ*M* (see text), the gray region illustrates the relatively narrow window of HMP partner concentrations available for analysis of PPIs by thermal shift.

$$\Delta^{L}G_u(T,[P],[L]) = \Delta^{apo}G_u(T) - \Delta G_b(T,[P],[L]), \quad (4)$$

where Δ^{apo} $G_u(T)$ is given by Eq. (13), and the binding free energy is as follows:

$$\Delta G_b = -RT\ln Q, \quad (5)$$

where Q is the binding polynomial of the partners.[31] For a single binding site at a concentration of P such that $[P] \ll [L]$, this becomes

$$\Delta G_b([L]) = -RT\ln\left(1+\frac{[L]}{K_d(T)}\right), \quad (6)$$

where $K_d(T)$ is the dissociation constant at temperature T. From this equation, it is readily apparent that isothermal free energies of binding increase continuously with $[L]$ (Fig. 2). In principle, this means that free energies can be measured over a very wide concentration range, which is one of the advantages of this method. In practice, however, there is an upper limit of protein concentrations that can be used for three reasons: (a) scale of protein production; (b) protein aggregation at high concentrations; and (c) masking of the signal reporting on the unfolding of the LMP by background signal from high concentrations of HMP. There is also a lower limit of protein concentrations that can be used in PPI thermal shift assays, which will usually be set by binding stoichiometry. As $[L]$ approaches a regime in which binding stoichiometry must be explicitly considered ($[L] < \sim 10\times[P]$), ΔG_b varies as given in Ref. 28:

$$\Delta G_{\mathrm{b}}(T,[P],[L]) = -RT\ln\left(1+\frac{[L]-[P]-2K_{\mathrm{d}}(T)+\sqrt{((L)+[P]+2K_{\mathrm{d}}(T))^2-4[P][L]}}{2K_{\mathrm{d}}(T)}\right), \quad (7)$$

where $[P]$ and $[L]$ are the *total* LMP and HMP concentrations, respectively. In this concentration range, ΔG_{b} deviates from Eq. (6) (Fig. 2, dashed lines). Although stoichiometric effects can be accounted for with Eq. (7), in this range, ΔG_{b} values are very sensitive to small errors in estimates of $[P]$ (i.e., the LMP concentration). It is, therefore, advisable to perform the experiment at $[L]$ (i.e., the HMP concentration) above the stoichiometric limit. For example, many proteins display good signal-to-noise ratio at concentrations of 1–6 μM in SO-monitored thermal unfolding, which establishes the range for $[P]$. To be above the stoichiometric regime, $[L]$, therefore, must be $\sim$ 10–60 μM. Between the stoichiometric lower limit and the practical upper limit, there may be a relatively narrow window of partner concentrations that can be used in a PPI thermal stability shift assay (Fig. 2). However, one significant property of measuring affinities by stability shifts is that if HMP concentration is above the stoichiometric regime and above the K_{d} (and there is no binding of N_{HMP} to D_{LMP}), affinities can be estimated from the magnitude of thermal shift at a single partner concentration.

Affinities are reported in terms of the dissociation constant, K_{d}. Because the observations that are used to determine affinity are made at varying temperatures, the temperature dependence of K_{d} must be considered explicitly, and it is given by

$$K_{\mathrm{d}}(T) = K_{\mathrm{d}}^{o} e^{\left[\frac{\Delta H_b^o}{R}\left(\frac{1}{T}-\frac{1}{T^o}\right)-\frac{\Delta C_{p,b}}{R}\left(\frac{T^o}{T}-1+\ln\left(\frac{T}{T^o}\right)\right)\right]}, \quad (8)$$

where $\Delta C_{p,\mathrm{b}}$ is the heat capacity of binding, and K_{d}^{o} and ΔH_b^o are the dissociation constant and the enthalpy of binding, respectively, at an arbitrary reference temperature T^o (see Materials and Methods section for derivation).

To construct a master equation that solves for K_{d}^{o}, we note that at the ligand-shifted T_{m} ($^{L}T_{\mathrm{m}}$) induced by some concentration, $[L]$, of ligand, the following relationship is true [from Eq. (4), shown here with all relevant input parameters]:

$$\Delta G_{\mathrm{u}}({}^{L}T_{\mathrm{m}}, {}^{\mathrm{apo}}T_{\mathrm{m}}, \Delta^{\mathrm{apo}}_{\mathrm{m}}H_{\mathrm{u}}, \Delta C_{p,\mathrm{u}}) - \Delta G_{\mathrm{b}}({}^{L}T_{\mathrm{m}}, T^o, K_{\mathrm{d}}^{o}, \Delta H_b^o, \Delta C_{p,b}, [L], [P]) = \Delta^{L}G_{\mathrm{u}} = 0 \quad (9)$$

where ΔG_{u} is described by the Gibbs–Helmholtz relationship [Eq. (3)],[28] and ΔG_{b} is described by Eqs. (7) and (8) ("apo" superscripted parameters describe thermal denaturation in the absence of ligand). Equation (9) can be solved numerically using Levenberg–Marquardt nonlinear minimization. We incorporate this minimization into a Monte Carlo method that fits unknown parameters many times over from randomly chosen initial values to discover the distribution of K_{d} values that are consistent with the observed binding-induced T_{m} shifts. In each Monte Carlo trial, experimentally measured parameters are sampled within the experimental error, and unknown parameters are fit from random initial values sampled from distributions reported in the literature.[32] Specifically, the $^{\mathrm{apo}}T_{\mathrm{m}}$ and $\Delta^{\mathrm{apo}}_{\mathrm{m}}H_{\mathrm{u}}$ values are experimentally determined by fitting the denaturation of the apoprotein,[28] $\Delta C_{p,\mathrm{u}}$ is calculated from the size of the apoprotein,[33] and $^{L}T_{\mathrm{m}}$ is determined as the minimum of the inverse derivative trough of the LMP unfolding transition in the presence of its binding partner (Fig. 3). In each trial, these four values are sampled from normal distributions defined by the mean and standard deviation of experimental replicates ($^{\mathrm{apo}}T_{\mathrm{m}}$, $\Delta^{\mathrm{apo}}_{\mathrm{m}}H_{\mathrm{u}}$, and $^{L}T_{\mathrm{m}}$) or by the error associated with the calculation of $\Delta C_{p,\mathrm{u}}$.[33] Following the choice of these values, $\Delta H_{\mathrm{b}}^{o}$ and $\Delta C_{p,\mathrm{b}}$ are fit along with K_{d}^{o} using the Levenberg–Marquandt algorithm. In each minimization trial, initial values for these parameters were generated by sampling $\Delta H_{\mathrm{b}}^{o}$, $\Delta C_{p,\mathrm{b}}$, and K_{d}^{o} obtained from normal distributions constructed from all proteins characterized by isothermal titration calorimetry at 25°C as shown in Ref. 32 [$\mu(\sigma)$: $\Delta H_{\mathrm{b}}^{o}$, −9 (14) kcal/mol; $\Delta C_{p,\mathrm{b}}$, −350 (250) Kcal/mol; K_{d}^{o} by Eq. (15) from $\Delta G_{\mathrm{b}}^{o}$, −9.9 (2.7)]. In this calculation, 25°C was used as the reference temperature (T^o). Trials that failed to converge [$\Delta^{L}G_{\mathrm{u}} = 0 \pm 1\mathrm{E}{-9}$, Eq. (19)] after a specified number of iterations of the minimization algorithm were discarded. The fit values of the $\Delta H_{\mathrm{b}}^{o}$, $\Delta C_{p,\mathrm{b}}$, and K_{d}^{o} parameters were used with Eq. (7) to finely sample and record K_{d} as a function of temperature over the range 0–100°C for each trial. We combine the results of many trials to construct a temperature-dependent distribution of $K_{\mathrm{d}}(T)$ (e.g., Fig. 4). After enough trials have been performed such that means and standard deviations are stable (we perform 500 successfully converging trials), we report the resulting distribution of K_{d} values at each temperature.

The stochastic method provides a quantitative evaluation of the error of the fits. Figure 4 shows the distribution of fits for the wild-type MBP–Off7 interaction (see "Experimental case study: MBP and a synthetic ankyrin repeat protein" section for more

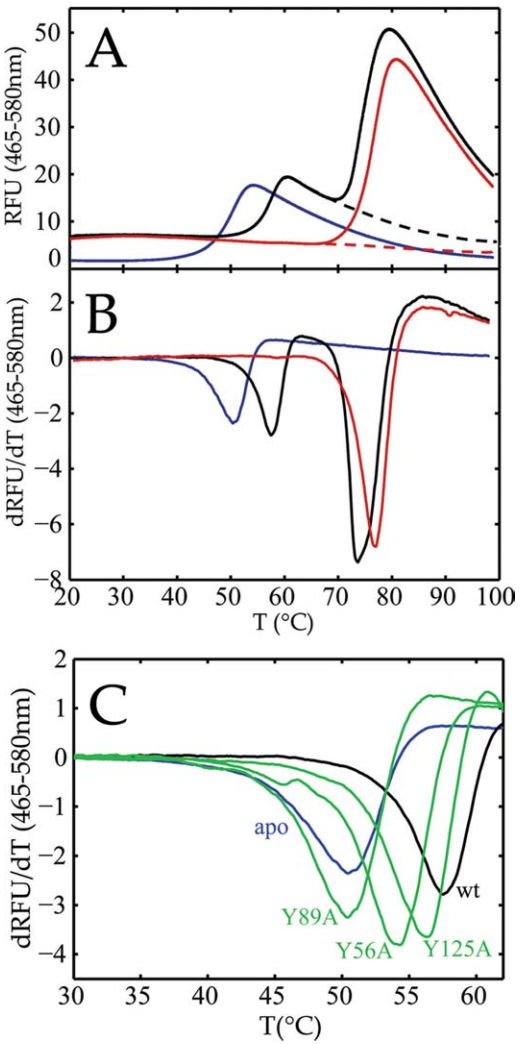

Figure 3. Experimental thermal unfolding curves of wild-type MBP (LMP) and Off7 (HMP) variants monitored with SO. (A) Fluorescence emission intensity of 2 μ*M* MBPwt only (blue), 25 μ*M* Off7wt only (solid red), and 2 μ*M* MBPwt combined with 25 μ*M* Off7wt (solid black). Note the shift in the LMP unfolding transition. Approximate extrapolated pre-HMP-transition baselines (dashed lines) are shown to qualitatively illustrate convolution of the signal reporting on the unfolding transitions. We interpret the skew (apparent in the first derivative plot) of the Off7 (HMP) unfolding transition in the presence of MBP as arising largely from this convolution, with a possible additional contribution by irreversible aggregation processes that may occur in the presence of denatured MBP. (B) Inverse first derivative plots of the unfolding curves in A. (C) Inverse first derivative plots of the LMP (2 μ*M* MBPwt) unfolding transitions in the presence of four Off7 variants (25 μ*M*; mutations indicated). All observations were made at 20× SO.

detail), reported as the temperature dependence of the K_d. Despite large uncertainties in many of the parameters, the K_d is quite well determined near the temperature at which ligand-shifted T_m values are observed in the experiments. Even without any specific information about ΔH°_b and $\Delta C_{p,b}$, a robust estimate of K_d is obtained near the temperature where the experimental data were collected. Unsurprisingly, the further the $K_d(T)$ is extrapolated away from the experimental regime, the larger the divergence of the curves. This behavior defines the utility and limitations of the method to determine affinities. It obtains quite precise data within the temperature range of the observations, but it should be used with great caution to make extrapolations over large temperature ranges. The method is, therefore, best suited for comparative studies, such as the effect of mutation on binding interactions, as presented in this study.

Experimental case study: MBP and a synthetic ankyrin repeat protein

The high-affinity interaction between MBP and the synthetic ankyrin repeat protein Off7 provides an

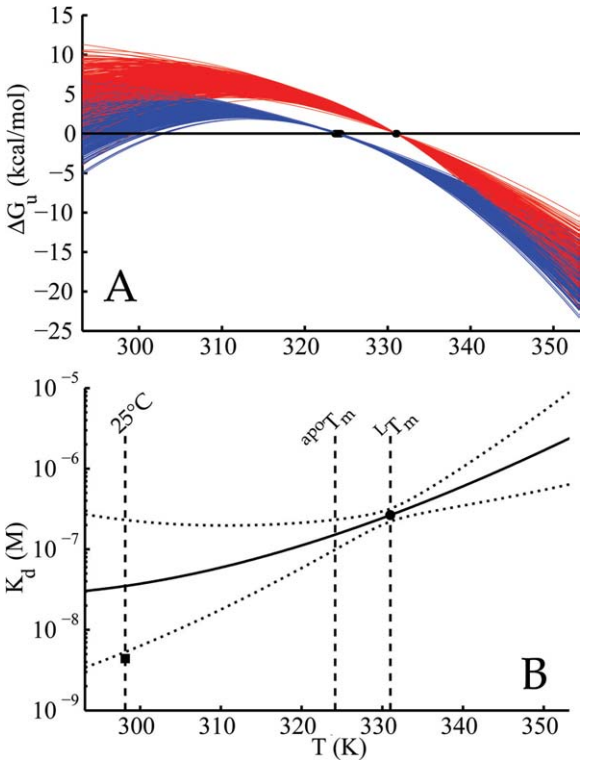

Figure 4. Fit to the thermodynamic model of experimental thermal shift data for the interaction between MBPwt and Off7 wt. (A) 500 Monte Carlo trials that fit MBP T_m values in the absence and presence of 25 μ*M* Off7 (filled circles). Each trial generates a temperature-dependent model of apo MBP stability [Eq. (3); blue] and Off7-shifted MBP stability [Eqs. (3), (4), (7), and (8); red] using parameters that were experimentally determined or randomly sampled from literature ranges as described in the text. (B) The temperature dependence of K_d values and error. The mean (solid black line) and one standard deviation (dotted black line) lines were determined at each temperature from the distribution of individual fits (panel A) at that temperature. The K_d value is most certain at the Off7-shifted $^{L}T_m$ (filled circle). The affinity of the interaction at 25°C as measured by surface plasmon resonance[27] is shown for comparison (4.4 n*M*, filled square). Affinities of all mutants in this study were reported at a common reference temperature, the $^{apo}T_m$ of MBP (51°C).

Table I. *Stability Shifts and Affinities for the Interactions Between Alanine Variants of MBP and Off7*[a]

MBP variant	Off7 variant	ΔΔTm	at 324K (51°C) ΔΔGb (kcal/mol)	at 324K (51°C) Kd (μM)	at 324K (51°C) ΔGb	at 298K (25°C) Kd (μM)	at 298K (25°C) ΔGb	apo MBP Tm	apo MBP ΔHu	MBP variant in the presence of Off7 variant Tm	ΔTm	apo Off7 Tm	apo Off7 ΔHu
					-10.1		-10		112.7		7.1	350.5	145.9
wt	wt	-	-	0.15 (0.10-0.23)	(0.26)	0.04 (0.006-0.2)	(1.1)	324.0 (0.11)	(0.67)	331 (0.03)	(0.12)	(0.13)	(0.61)
		-7.7									-0.6	337.6	132
wt	D77A	(0.16)	>4	>~100μM	-	-	-			323.5 (0.09)	(0.11)	(0.04)	(0.27)
		-7.6									-0.5	355.2	132.7
wt	W90A	(0.15)	>4	>~100μM	-	-	-			323.5 (0.07)	(0.08)	(0.01)	(1.13)
		-7.3									-0.2	348.2	132.1
wt	Y89A	(0.20)	>4	>~100μM	-	-	-			323.8 (0.12)	(0.16)	(0.04)	(0.3)
		-6.6			-6.0		-6.6				0.5	346.1	98.0
wt	Y81A	(0.15)	4.1 (0.30)	97 (76-120)	(0.15)	10 (2-100)	(1.2)			324.4 (0.05)	(0.08)	(0.05)	(0.83)
		-6.6			-6.2		-6.8				0.5	334.6	98.7
wt	F79A	(0.19)	3.9 (0.33)	64 (47-87)	(0.20)	10 (1-70)	(1.2)			324.6 (0.11)	(0.14)	(0.05)	(0.80)
		-5.4			-7.2		-7.8				1.7	354.3	118.2
wt	W123A	(0.20)	2.9 (0.29)	13 (11-16)	(0.13)	2 (0.3-10)	(1.2)			325.8 (0.16)	(0.16)	(1.24)	(0.17)
		-5.3			-7.3		-7.8				1.8	345.6	107.6
wt	L86A	(0.22)	2.8 (0.30)	11 (9.2-14)	(0.14)	2 (0.3-10)	(1.2)			325.8 (0.16)	(0.18)	(0.16)	(2.16)
		-4.6			-7.8		-8.3				2.5	355.2	140.3
wt	D110A	(0.18)	2.3 (0.30)	5.6 (4.5-7.1)	(0.15)	0.8 (0.09-7)	(1.3)			326.6 (0.13)	(0.13)	(0.04)	(0.18)
		-3.9			-8.2		-8.7				3.2	354.3	121.8
wt	Y56A	(0.15)	1.9 (0.30)	3.0 (2.4-3.8)	(0.15)	0.4 (0.05-3)	(1.2)			327.4 (0.03)	(0.09)	(0.02)	(0.72)
		-1.9			-9.2		-9.5				5.2	344.2	81.9
wt	Y125A	(0.15)	0.9 (0.35)	0.62 (0.43-0.90)	(0.24)	0.1 (0.01-0.9)	(1.2)			329.3 (0.08)	(0.09)	(0.02)	(0.09)
		-1.5			-9.4		-9.6				5.6	349.3	131.5
wt	D112A	(0.20)	0.7 (0.35)	0.48 (0.33-0.70)	(0.24)	0.09 (0.01-0.6)	(1.1)			329.3 (0.16)	(0.16)	(0.02)	(1.22)
		-0.4			-10.0		-10				6.7	349.6	207.8
wt	T48A	(0.19)	0.1 (0.39)	0.19 (0.12-0.30)	(0.29)	0.04 (0.006-0.3)	(1.2)			330.8 (0.05)	(0.15)	(0.03)	(0.51)
		-6.4			-6.2		-6.8				0.7	350.5	145
H203A	wt	(0.13)	3.9 (0.27)	66 (60-73)	(0.07)	10 (2-60)	(1.1)	322.1 (0.01)	101.4 (0.03)	322.8 (0.03)	(0.03)	(0.22)	(1.9)
		-5.8			-6.8		-7.4				1.3		
K200A	wt	(0.15)	3.3 (0.27)	27 (24-30)	(0.07)	4 (0.6-20)	(1.1)	322.2 (0.01)	105.8 (0.22)	323.5 (0.09)	(0.09)		
		-5.5			-7.0		-7.6				1.6		
K202A	wt	(0.22)	3.1 (0.29)	20 (16-24)	(0.13)	2 (0.4-20)	(1.2)	322.7 (0.03)	103.5 (0.50)	324.3 (0.18)	(0.18)		
		-4.9			-7.3		-7.9				2.2		
D136A	wt	(0.72)	2.8 (0.56)	12 (5.6-26)	(0.50)	2 (0.2-10)	(1.2)	321.8 (0.7)	102.5 (3.2)	324.0 (0.09)	(0.71)		
		-4.7			-7.7		-8.2				2.4		
K137A	wt	(0.15)	2.4 (0.28)	6.7 (5.7-8.1)	(0.11)	1 (0.1-9)	(1.3)	323.8 (0.01)	110.9 (0.78)	326.2 (0.08)	(0.08)		
		-1.5			-9.2		-9.5				5.6		
K140A	wt	(0.15)	0.9 (0.32)	0.58 (0.43-0.78)	(0.19)	0.1 (0.01-0.8)	(1.2)	322.5 (0.07)	106.2 (1.29)	328.1 (0.04)	(0.08)		
		-1.6			-9.2		-9.5				5.5		
N201A	wt	(0.19)	0.9 (0.33)	0.59 (0.43-0.81)	(0.20)	0.1 (0.01-0.8)	(1.2)	322.6 (0.03)	109.2 (0.95)	328.1 (0.14)	(0.14)		
		1.6			-10.9		-10.5				8.7		
D197A	wt	(0.16)	-0.8 (0.37)	0.046 (0.031-0.070)	(0.26)	0.02 (0.004-0.1)	(1.0)	321.3(0.1)	111.9 (0.89)	330.0 (0.02)	(0.10)		

[a] Standard deviations indicated in parentheses.

appropriate test case for the method presented in this work because the T_m values of the two partners are well separated. We observe a significant shift of the T_m value of MBP (the LMP) in the presence of Off7 (the HMP) [Fig. 3(A)]. The K_d of the interaction between MBP and Off7 was originally determined to be 4.4 nM by surface plasmon resonance (SPR) at 25°C.[30] When the affinity is measured by thermal stability shift analysis, the uncertainty in the result is lowest at the ${}^{L}T_m$ (58°C), where the affinity is found to be 260 nM within one standard deviation (1σ) of (220–320 nM).

Using a series of alanine mutations constructed by site-directed mutagenesis of residues in the interface region of either partner, we demonstrate that it is possible to quantitate affinities over several orders of magnitude. K_d values were estimated from thermal unfolding shifts in the MBP variant observed in the presence and absence of the Off7 variant at 25 μM. An added benefit of this approach is that it can also readily be used to assess the effect of mutation on the stability of each partner individually (Table I). Due to the temperature dependence of binding, in comparative analysis of affinities between various partners ($\Delta\Delta G_b$ values), affinities must be reported at the same temperature. We compare affinities at the MBPwt ${}^{apo}T_m$ (51°C), where K_d is relatively well determined for all mutants, and report $\Delta\Delta G_b$ values for all variant pairs at this temperature. T_m for both partners is also reported. The residue numbering used in the identification of mutations is taken from the structure of the complex PDBID 1SVX.

Comparison of the affinities measured by thermal shift to values obtained by other methods at very different temperatures should be done with caution because of the difficulties in extrapolating too far between temperatures (see above). The affinity of the interaction between MBP and Off7 has been determined by SPR to be 4.4 nM at 25°C, with an unreported error.[30] The mean of the extrapolated affinities is 40 nM at this temperature, with a large uncertainty (1σ = 6–200 nM). The two observations are consistent in that they fall approximately within each other's experimental error and that the affinity decreases with temperature. No corresponding SPR data are available for the mutants reported in this study, limiting quantitative corroboration. However, the rank ordering of these mutant affinities is consistent with that obtained by a semiquantitative method.[34]

Equilibrium conditions

It is essential that the system be in equilibrium if the thermodynamic model presented in this study is to be applied. Equilibration can be probed using an isothermal dwell period programmed into the RT-PCR instrument near the T_m of the LMP, which is MBP is this case.[28] Empirical optimization revealed

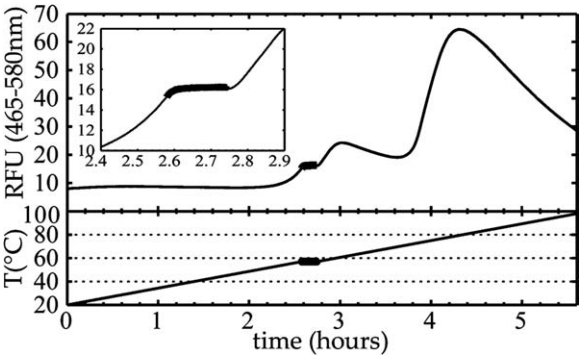

Figure 5. Isothermal dwell to test whether the ramp rate is sufficiently slow to allow equilibration of the system in the LMP unfolding transition region. The temperature is held constant near the T_m of the LMP (thick black). The minimal signal change over the isothermal period indicates equilibrium (see inset). Using this test, the ramp rate was empirically optimized to 0.239°C/min. The unfolding experiment takes several hours at this ramp rate.

that a rate of 0.239°C/min was necessary for equilibrium unfolding of MBP in the presence of Off7, and this rate was used for all experiments in this study (Fig. 5). Data acquisition, therefore, required almost 6 h to complete. Even at these slow ramp rates, simultaneous collection of unfolding data for 384 samples are still quite high throughput in comparison to conventional methods for measuring stability or PPI interactions.

SO concentration-dependent effects

The mechanism whereby SO reports on unfolding remains poorly understood.[28] Models (including the one presented in this study) used to interpret the data assume that SO is an inert reporter of protein unfolding that does not inhibit binding interactions or (de)stabilize protein. However, we have shown previously that SO can perturb unfolding equilibria, thereby affecting derived thermodynamic parameters such as T_m values and binding free energies.[28] To investigate to what extent SO affects the MBP–Off7 PPI, we performed a series of thermal shift assays at a series of SO concentrations (Fig. 6). From these observations, it is clear that there is a significant destabilization (lowering of the apparent T_m) of MBP by SO as observed previously.[28] However, in the lower concentration range of SO (~ 7 to ~ 35×)* the effect on K_d values is quite small. We have chosen 20× SO as the standard concentration to obtain our measurements because this concentration reports on unfolding with excellent signal-to-noise ratio and falls within this stable range.

*The formula and molar concentration of SYPRO Orange is not disclosed. Therefore, arbitrary units of "x" are used as provided by the manufacturer.

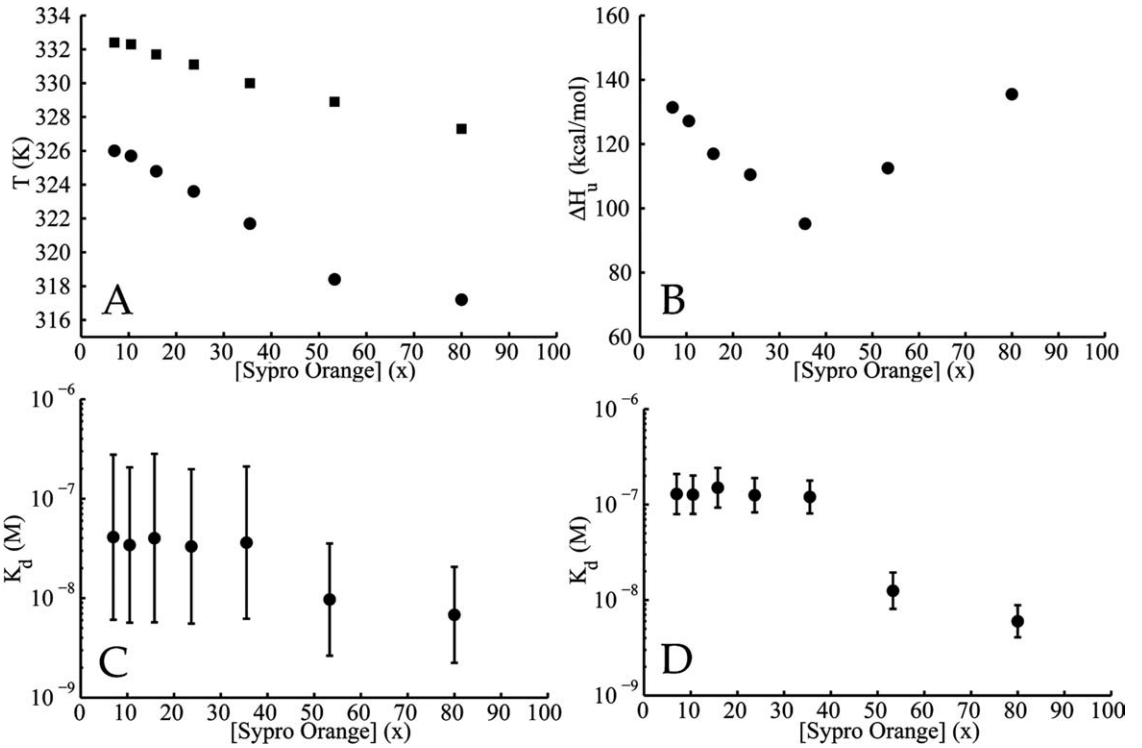

Figure 6. Dependence of the interaction between MBPwt and Off7wt on SO concentration. (A) T_m values of apo MBP (filled circles) and MBP in the presence of Off7 (filled squares). (B) ΔH_u values of apo MBP. (C) K_d values reported at 25°C. (D) K_d values reported at the $^{apo}T_m$ of MBP (51°C).

Conclusions

We have demonstrated that PPIs can be detected and quantified by analysis of shifts in thermal stability of a protein in the presence of its binding partner. Data collection is rapid and straightforward using readily available RT-PCR instrumentation. Unlike methods that determine the fraction complex formation as a function of ligand concentration, this method does not necessarily require the construction of a titration series that brackets the dissociation constant. Within the limiting assumptions of the thermodynamic model used in this study to analyze the experimental data, information can be obtained at any protein concentration above the stoichiometric limit and dissociation constant. High experimental throughput is enabled both by sample parallelization in microtiter plates and by the ability to extract quantitative binding information at a single concentration of the HMP. The experiments are carried out in 384-well microtiter plates with 20-μL sample volumes, requiring only picomoles of protein. In a single experiment, we have been able to quantify the affinities of a series of mutant interfaces, covering a relatively wide range of affinities ($\sim$ 100 nM to $\sim$ 100 μM at 51°C).

Binding affinities are inherently temperature dependent. Affinities measured using ligand-dependent shifts in thermal stability will generally need to take this dependence into account because experimental observations are made at different T_m values. The numerical method presented in this study for estimating affinities from thermal stability shifts empirically illustrates the temperature dependence of the error in such extrapolations. Although the temperature dependence of binding is dependent on a number of parameters that are absent or ill-determined from thermal stability shift analysis, we find that the affinity is well determined near the $^{L}T_m$, but it becomes increasingly uncertain upon extrapolation. This implies that the effect of mutations on binding can be evaluated with reasonable confidence at temperatures near the T_m in studies of protein–protein interfaces, but that extrapolation to physiological or other experimental conditions should be made with considerable caution.

As is the case for the analysis of interactions with small molecules, quantitation of PPIs by this method needs to take into account equilibration times and SO-dependent effects. Equilibration conditions are established experimentally by systematically exploring temperature ramp rates. The models used to interpret the data assume that SO is an inert reporter of protein unfolding. However, as shown previously, SO can significantly perturb the (un)folding and binding equilibria on which it is reporting.[28] The use of SO may, therefore, introduce systematic errors. The method and thermodynamic framework, which we have presented in this study,

is not limited to the use of SO dye but can be applied to any experimental signal for thermal protein unfolding.

We have been able to demonstrate that PPIs can be quantified using thermal stability shift measurements by taking advantage of the fact that the T_m values of MBP and Off7 are sufficiently well separated such that the thermodynamics of this interaction can be analyzed solely in terms of the effects of the latter on the stability of the former.

Quantitative determination of PPI affinities is a difficult experimental challenge. Although a number of methods have been developed,[10–17] all rely on the measurement of physical observables (e.g., heat, fluorescence, change in thermal stability), each with unique intrinsic limitations. The class of methods that determine equilibria by measuring the fraction of complex formation (e.g., fluorescence-based titrations) require that the concentration of the partner being titrated is both super-stoichiometric and brackets the K_d value. These constraints limit their applicability for the measurement of high-affinity interactions, as the protein concentrations become too low for signal detection. Fluorescence-based methods also may require labeling, which is not always straightforward.[12,13] SPR relies on immobilization of one of the partners, which can introduce steric hinderances to binding based on the geometry of immobilization or induce unfolding and promote nonspecific interactions. Identification of a suitable scheme for surface immobilization for each individual protein to be analyzed is, therefore, both nontrivial and critical to the generation of meaningful SPR data.[35] Methods that exploit partner-induced stability shifts, such as reported in this study, do not require matching protein concentrations with K_d values, provided that the concentrations are super-stoichiometric and are in excess of the K_d. Such methods are, therefore, particularly well suited to measure high-affinity interactions. In case where such binding-induced stability shifts are measured in an RT-PCR machine, the data are remarkably easy to collect and are amenable to high-throughput analysis in multiwell microtitration plates. A disadvantage is that analysis of binding based on thermal denaturation requires the development of an intricate thermodynamic model and that the resulting binding free energies are determined at elevated temperatures, necessitating the use of extrapolation if physiological temperatures are needed. Not every PPI can be analyzed by these means. For instance, thermophilic proteins may not denature within an experimentally accessible temperature range. The analysis presented in this study further requires that the T_m values of the partners are well separated. With further development, the thermodynamic framework and signal processing methods used in this work can be extended to a general analysis of PPIs that does not require nonoverlap of folding transitions. These methods are well suited for a rapid comparative thermodynamic analysis of the effects of interfacial mutations, such as the one reported in this study.

Materials and Methods

Genetic constructs and protein purification

Off7 and MBP variants were assembled from oligonucleotides[36] into full-length linear genes including T7 promoter, ribosomal binding site (RBS), T7 terminator, and restriction sequences. The wild-type Off7 open reading frame DNA sequence was optimized computationally for expression[37] and minimization of direct sequence repeats to facilitate PCR assembly of this repeat protein (see supplementary materials for sequences). Genes were cloned into pUC19 (NEB N3041L), and sequence was verified. Plasmids were transformed into Promega KRX cells (Promega L3002) in 96-well format (heat shock at 42°C was carried out in a 96-well PCR machine) and plated on carbenicillin (50 mg/mL) agar plates. Single colonies were picked and used to inoculate 6 mL of autoinduction media[38] containing 0.1% rhamnose in 96-well growth format. After 24 h growth at 37°C, cells were pelleted, resuspended, and lysed in 300-μL BugBuster (Novagen 71456). After lysis, cell debris was pelleted, and the supernatant decanted and incubated for 30 min at 4°C with His-binding gel (Sigma P6611, 100 μL of the 50% slurry for Off7 variants or 200 μL for MBP variants) with gentle shaking. To wash, resin was resuspended in cold wash buffer (50 m*M* sodium phosphate, 300 m*M* NaCl, 7.5 m*M* imidazole, pH 7.5) for 1 min with gentle mixing, then spun down and the supernatant carefully removed with a multichannel vacuum device (IBS Integra Biosciences). Following five washes, protein was eluted off the resin by incubating in 100 μL elution buffer (50 m*M* sodium phosphate, 300 m*M* NaCl, 300 m*M* imidazole, pH 7.8) for 30 minutes at 4°C with gentle shaking. Protein eluate was then exchanged into assay buffer (25 m*M* potassium phosphate, 140 m*M* KCl, pH 7.5) in a 96-well desalting plate (Pierce 89807). This high-throughput protein purification procedure routinely yields 75–300 μ*M* protein at 100 μL scale for Off7 and MBP variants. All assays reported in this study were performed in this assay buffer with 20× SO unless otherwise stated.

Derivation of the temperature dependence of K_d

Under the assumption of temperature independence of the heat capacity of a binding interaction, $\Delta C_{p,b}$ (note that it is unclear how justified this assumption is for binding[32]), the temperature dependence of the enthalpy of binding can be described as follows[39]:

$$\Delta H_{\mathrm{b}}(T) = \Delta H_{\mathrm{b}}^{o} - \int_{T}^{T^{o}} \Delta C_{p,b}\mathrm{d}T = \Delta H_{\mathrm{b}}^{o} - \Delta C_{p,b}(T^{o} - T) \tag{10}$$

where $\Delta H_{\mathrm{b}}(T)$ and $\Delta H_{\mathrm{b}}^{o}$ are the enthalpies of binding at temperature T and the reference temperature T^{o}, respectively. Similarly, for the temperature dependence of the entropy of binding, ΔS_{b}:

$$\Delta S_{b}(T) = \Delta S_{b}^{o} - \int_{T}^{T^{o}} \frac{\Delta C_{p,b}}{T} dT = \Delta S_{b}^{o} + \Delta C_{p,b}\ln\left(\frac{T}{T^{o}}\right) \tag{11}$$

If we know the free energy of binding, $\Delta G_{\mathrm{b}}^{o}$, at the reference temperature T^{o}, we can use the relationship

$$\Delta G_{b}^{o} = \Delta H_{b}^{o} - T^{o}\Delta S_{b}^{o} \tag{12}$$

to describe $\Delta S_{\mathrm{b}}^{o}$ in terms of $\Delta H_{\mathrm{b}}^{o}$

$$\Delta S_{b}^{o} = \left(\frac{\Delta H_{b}^{o} - \Delta G_{b}^{o}}{T^{o}}\right) \tag{13}$$

and substitute this to obtain an expression for the temperature dependence of ΔG_{b} in terms of ΔH_{b} and $\Delta C_{p,\mathrm{b}}$ (the Gibbs–Helmholtz relationship):

$$\Delta G_{b}(T) = \Delta H_{b}^{o} - \left(\frac{T}{T^{o}}\right)(\Delta H_{b}^{o} - \Delta G_{b}^{o}) - \Delta C_{p,b}\left(T^{o} - T + T\ln\left(\frac{T}{T^{o}}\right)\right) \tag{14}$$

Now, given that

$$\Delta G_{b}^{o} = RT^{o}\ln(K_{d}^{o}) \tag{15}$$

where K_{d}^{o} is the dissociation constant at T^{o} and that

$$\Delta G_{b}(T) = RT\ln(K_{d}(T)) \tag{16}$$

At any temperature T, we have [from Eqs. (5)–(7)]:

$$RT\ln(K_{d}(T)) = \Delta H_{b}^{o} - \left(\frac{T}{T^{o}}\right)(\Delta H_{b}^{o} - RT^{o}\ln(K_{d}^{o})) - \Delta C_{p,b}\left(T^{o} - T + T\ln\left(\frac{T}{T^{o}}\right)\right) \tag{17}$$

which simplifies to

$$\ln(K_{d}(T)) = \frac{\Delta H_{b}^{o}}{R}\left(\frac{1}{T} - \frac{1}{T^{o}}\right) - \frac{\Delta C_{p,b}}{R}\left(\frac{T^{o}}{T} - 1 + \ln\left(\frac{T}{T^{o}}\right)\right) + \ln(K_{d}^{o}) \tag{18}$$

or

$$K_{d}(T) = K_{d}^{o}e^{\left[\frac{\Delta H_{b}^{o}}{R}\left(\frac{1}{T} - \frac{1}{T^{o}}\right) - \frac{\Delta C_{p,b}}{R}\left(\frac{T^{o}}{T} - 1 + ln\left(\frac{T}{T^{o}}\right)\right)\right]} \tag{19}$$

Note that this is a similar but not identical to an equation describing the temperature dependence of K_{d} published earlier.[18]

Monitoring of protein unfolding and protein–protein binding with SO

Experimental observations of protein unfolding were made by monitoring SO fluorescence measurements on a Roche LightCycler 480 II RT-PCR machine with filters to excite at 465 nm and measure emission at 580 nm as temperature was continuously increased at a ramp rate of 0.239°C/min. Samples of each MBP variant at a final concentration of 2 μM were unfolded in the presence or absence of Off7 variants at 25 μM. Each sample was subdivided into either two or four 20 μL replicates on a 384-well plate. Experimental replicates were independently fit and analyzed as described above.

Numerical analysis

Fits of the experimental data to the thermodynamic model using Levenberg–Marquardt nonlinear minimization and Monte Carlo sampling of parameters were implemented in MATLAB.

References

1. Ptashne M (2009) Binding reactions: epigenetic switches, signal transduction and cancer. Curr Biol 19:234–241.
2. Pawson T, Nash P (2003) Assembly of cell regulatory systems through protein interaction domains. Science 300:445–452.
3. Jeong H, Mason SP, Barabási AL, Oltvai ZN (2001) Lethality and centrality in protein networks. Nature 411:41–42.
4. Rual J-F, Venkatesan K, Hao T, Hirozane-Kishikawa T, Dricot A, Li N, Berriz GF, Gibbons FD, Dreze M, Ayivi-Guedehoussou N, Klitgord N, Simon C, Boxem M, Milstein S, Rosenberg J, Goldberg DS, Zhang LV, Wong SL, Franklin G, Li S, Albala JS, Lim J, Fraughton C, Llamosas E, Cevik S, Bex C, Lamesch P, Sikorski RS, Vandenhaute J, Zoghbi HY, Smolyar A, Bosak S, Sequerra R, Doucette-Stamm L, Cusick ME, Hill DE, Roth FP, Vidal M (2005) Towards a proteome-scale map of the human protein-protein interaction network. Nature 437:1173–1178.
5. Wells JA, McClendon CL (2007) Reaching for high-hanging fruit in drug discovery at protein-protein interfaces. Nature 450:1001–1009.
6. Schoeberl B, Pace EA, Fitzgerald JB, Harms BD, Xu L, Nie L, Linggi B, Kalra A, Paragas V, Bukhalid R, Grantcharova V, Kohli N, West Ka, Leszczyniecka M, Feldhaus MJ, Kudla AJ, Nielsen UB (2009) Therapeutically targeting ErbB3: a key node in ligand-induced activation of the ErbB receptor-PI3K axis. Sci Signal 2:ra31.
7. Clackson T, Wells JA (1995) A hot spot of binding energy in a hormone–receptor interface. Science 267:383–386.
8. Pons J, Rajpal A, Kirsch JF (1999) Energetic analysis of an antigen/antibody interface: alanine scanning mutagenesis and double mutant cycles on the HyHEL-10/lysozyme interaction. Protein Sci 8:958–968.
9. Schreiber G, Fersht AR (1995) Energetics of protein-protein interactions: analysis ofthe Barnase–Barstar

interface by single mutations and double mutant cycles. J Mol Biol 248:478–486.
10. Boozer C, Kim G, Cong S, Guan H, Londergan T (2006) Looking towards label-free biomolecular interaction analysis in a high-throughput format: a review of new surface plasmon resonance technologies. Curr Opin Biotechnol 17:400–405.
11. Abdiche Y, Malashock D, Pinkerton A, Pons J (2008) Determining kinetics and affinities of protein interactions using a parallel real-time label-free biosensor, the Octet. Anal Biochem 377:209–217.
12. Brient-Litzler E, Plückthun A, Bedouelle H (2010) Knowledge-based design of reagentless fluorescent biosensors from a designed ankyrin repeat protein. Protein Eng Des Sel 23:229–241.
13. Sloan DJ, Hellinga HW (1998) Structure-based engineering of environmentally sensitive fluorophores for monitoring protein-protein interactions. Protein Eng 11: 819–823.
14. Yan Y (2003) Analysis of protein interactions using fluorescence technologies. Curr Opin Chem Biol 7:635–640.
15. Leavitt S, Freire E (2001) Direct measurement of protein binding energetics by isothermal titration calorimetry. Curr Opin Struct Biol 11:560–566.
16. Pierce MM, Raman CS, Nall BT (1999) Isothermal titration calorimetry of protein–protein interactions. Methods 19:213–221.
17. Darling RJ, Brault P-A (2004) Kinetic exclusion assay technology: characterization of molecular interactions. Assay Drug Dev Technol 2:647–657.
18. Pantoliano MW, Petrella EC, Kwasnoski JD, Lobanov VS, Myslik J, Graf E, Carver T, Asel E, Springer BA, Lane P, Salemme FR (2001) High-density miniaturized thermal shift assays as a general strategy for drug discovery. J Biomol Screen 6:429–440.
19. Lo M-C, Aulabaugh A, Jin G, Cowling R, Bard J, Malamas M, Ellestad G (2004) Evaluation of fluorescence-based thermal shift assays for hit identification in drug discovery. Anal Biochem 332:153–159.
20. Niesen FH, Berglund H, Vedadi M (2007) The use of differential scanning fluorimetry to detect ligand interactions that promote protein stability. Nat Protoc 2: 2212–2221.
21. Isom DG, Vardy E, Oas TG, Hellinga HW (2010) Picomole-scale characterization of protein stability and function by quantitative cysteine reactivity. Proc Natl Acad Sci USA 107:4908–4913.
22. Ghaemmaghami S, Fitzgerald MC, Oas TG (2000) A quantitative, high-throughput screen for protein stability. Proc Natl Acad Sci USA 97:8296–8301.
23. Park C, Marqusee S (2005) Pulse proteolysis: a simple method for quantitative determination of protein stability and ligand binding. Nat Methods 2:207–212.
24. West GM, Tang L, Fitzgerald MC (2008) Thermodynamic analysis of protein stability and ligand binding using a chemical modification- and mass spectrometry-based strategy. Anal Chem 80:4175–4185.
25. Senisterra GA, Finerty PJ (2009) High throughput methods of assessing protein stability and aggregation. Mol BioSyst 5:217–223.
26. Brandts JF, Lin LN (1990) Study of strong to ultratight protein interactions using differential scanning calorimetry. Biochemistry 29:6927–6940.
27. Isom DG, Marguet PR, Oas TG, Hellinga HW (2011) A miniaturized technique for assessing protein thermodynamics and function using fast determination of quantitative cysteine reactivity. Proteins 79:1034–1047.
28. Layton CJ, Hellinga HW (2010) Thermodynamic analysis of ligand-induced changes in protein thermal unfolding applied to high-throughput determination of ligand affinities with extrinsic fluorescent dyes. Biochemistry 49:10831–10841.
29. Steinberg TH, Jones LJ, Haugland RP, Singer VL (1996) SYPRO Orange and SYPRO red protein gel stains: one-step fluorescent staining of denaturing gels for detection of nanogram levels of protein. Anal Biochem 239: 223–237.
30. Binz HK, Amstutz P, Kohl A, Stumpp MT, Briand C, Forrer P, Grütter MG, Plückthun A (2004) High-affinity binders selected from designed ankyrin repeat protein libraries. Nat Biotechnol 22:575–582.
31. Wyman J (1974) A probabilistic approach to cooperativity of ligand binding by a polyvalent molecule. Proc Natl Acad Sci USA 71:3431–3434.
32. Stites WE (1997) Protein-protein interactions: interface structure, binding thermodynamics, and mutational analysis. Chem Rev 97:1233–1250.
33. Myers JK, Pace CN, Scholtz JM (1995) Denaturant m values and heat capacity changes: relation to changes in accessible surface areas of protein unfolding. Protein Sci 4:2138–2148.
34. Layton CJ, Hellinga HW (2011) Integration of cell-free protein coexpression with an enzyme-linked immunosorbent assay enables rapid analysis of protein-protein interactions directly from DNA. Prot Sci 20:1432–1438.
35. Rich RL, Myszka DG (2000) Advances in surface plasmon resonance biosensor analysis. Curr Opin Biotechnol 11:54–61.
36. Cox JC, Lape J, Sayed MA, Hellinga HW (2007) Protein fabrication automation. Protein Sci 16:379–390.
37. Allert M, Cox JC, Hellinga HW (2010) Multifactorial determinants of protein expression in prokaryotic open reading frames. J Mol Biol 402:905–918.
38. Studier FW (2005) Protein production by auto-induction in high density shaking cultures. Protein Expr Purif 41:207–234.
39. Privalov PL, Khechinashvili NN (1974) A thermodynamic approach to the problem of stabilization of globular protein structure: a calorimetric study. J Mol Biol 86:665–684.